

# Molecular Dynamics Simulation of Molten Alkali Nitrates

G. Vöhringer and J. Richter

Institut für Physikalische Chemie der RWTH Aachen, Templergraben 59, D-52056 Aachen

Reprint requests to Prof. J. R.; Fax: +49-241-8888-235; E-mail: richter@rwth-aachen.de

Z. Naturforsch. **56 a**, 337–341 (2001); received April 2, 2001

Molecular dynamics (MD) simulations have been performed for several pure alkali nitrate melts. Special attention was paid to the examination of the interaction potential: macroscopic quantities like pressure were calculated and compared with real values. To improve the results the commonly used potential for alkali nitrates (Coulomb pair potential and Born-type repulsion) has been extended by a short-range-attraction term to meet the real behaviour of the liquid.

With these improved potentials, simulations of pure  $\text{LiNO}_3$ ,  $\text{NaNO}_3$ ,  $\text{KNO}_3$ , and  $\text{RbNO}_3$  have been performed with special regard to the influence of size and mass of the cations on the transport effects to show analogies to isotope effects. The calculated self diffusion coefficients (SDC) have been compared to results obtained with the NMR spin echo method.

**Key words:** Simulation; Molecular Dynamics; Interaction Potential; Alkali Nitrate; Melt.

## 1. Introduction

Only few molecular dynamics (MD) simulations on molten nitrates are reported until now [1–8]. Our experimental work [9–12] deals with transport coefficients of nitrate melts and their mixtures, especially diffusion coefficients. Therefore we performed MD simulations to interpret our experimental results, measured by the NMR spin echo method. The original objective was to establish a simulation of a mixture of  $^6\text{LiNO}_3$  and  $^7\text{LiNO}_3$ , because measurements with the mentioned method showed subtle differences in the transport coefficients between the two isotopes [10].

## 2. Molecular Dynamics Simulation

MD simulations were done on pure molten salts containing alkali ( $\text{Na}^+$ ,  $\text{Li}^+$ ,  $\text{K}^+$ , and  $\text{Rb}^+$ ) and  $\text{NO}_3^-$  ions. The side length  $L$  of our basic cell was determined by  $L = (N m / \rho)^{1/3}$ , where  $N$  is the number of ion pairs,  $m$  the mass of one sodium nitrate molecule and  $\rho$  the density at the specified temperature according to [13]. The time increment  $\Delta t$  was chosen to be either 2.5 or 5.0 fs. In the calculation of the Coulomb force the Ewald method [14] was used with the cut-off distance  $L/2$ . The summation in reciprocal space was taken up to  $|h|^2 = 27$  ( $h$  is the reciprocal lattice vector in units such that its components are integers), and the convergence parameter  $\kappa = 6.5/L$ . The nitrate

ion was treated as a rigid body, the rotational motion was expressed by quaternions and calculated by the algorithm proposed by Svanberg [15], which improves energy conservation. The intraatomic distance  $r_{\text{NO}}$  was 125 pm.

The time increment was 2.5 fs for simulations of  $\text{LiNO}_3$  and 5.0 fs for all other simulations. The system contained 216 ion pairs, and a typical simulation consisted of 20,000 time-steps for thermalisation, 20,000 steps of equilibration and finally 40,000 steps of gathering of the simulation data. All simulations were performed in the microcanonical ensemble.

The adopted pair potential  $V_{ij}$  consisted of the coulombic and repulsive Born-type terms:

$$V_{ij}(r) = \frac{z_i z_j e^2}{4\pi\epsilon_0 r} + \left(1 + \frac{z_i}{n_i} + \frac{z_j}{n_j}\right) b \exp\left(\frac{\sigma_i + \sigma_j}{\rho_{ij}} - \frac{r}{\rho_{ij}}\right). \quad (1)$$

$z_{i,j}$  is the ionic charge number of ion  $i$  or  $j$ ,  $e$  the elementary charge,  $\epsilon_0$  the permittivity of free space,  $n_{i,j}$  the number of electrons in the outer shell of ion  $i$  or  $j$ ,  $b$  a constant ( $3.38 \times 10^{-20}$  J),  $\sigma_{i,j}$  the ionic radius of ion  $i$  or  $j$ ,  $\rho_{ij}$  a “hardness parameter”, and  $r$  the distance between the ions  $i$  and  $j$ . The parameters were chosen so that the nitrate ion was represented by the  $\sigma_{i,j}$  and  $\rho_{i,j}$  parameters used by Yamaguchi

0932–0784 / 01 / 0500–0337 \$ 06.00 © Verlag der Zeitschrift für Naturforschung, Tübingen · www.znaturforsch.com



Dieses Werk wurde im Jahr 2013 vom Verlag Zeitschrift für Naturforschung in Zusammenarbeit mit der Max-Planck-Gesellschaft zur Förderung der Wissenschaften e.V. digitalisiert und unter folgender Lizenz veröffentlicht: Creative Commons Namensnennung-Keine Bearbeitung 3.0 Deutschland Lizenz.

Zum 01.01.2015 ist eine Anpassung der Lizenzbedingungen (Entfall der Creative Commons Lizenzbedingung „Keine Bearbeitung“) beabsichtigt, um eine Nachnutzung auch im Rahmen zukünftiger wissenschaftlicher Nutzungsformen zu ermöglichen.

This work has been digitalized and published in 2013 by Verlag Zeitschrift für Naturforschung in cooperation with the Max Planck Society for the Advancement of Science under a Creative Commons Attribution-NoDerivs 3.0 Germany License.

On 01.01.2015 it is planned to change the License Conditions (the removal of the Creative Commons License condition “no derivative works”). This is to allow reuse in the area of future scientific usage.

Table 1. Properties of the atoms.

Parameter	Li	Na	— Atom —			
			K	Rb	N	O
Charge number $z$	1	1	1	1	0.6599	-0.5533
Number $n$ of valence electrons	2	8	8	8	4.3401	6.5533
Radius $\sigma$ [pm]	87.5	117	140	145	70	105
Mass $m$ [ $10^{-26}$ kg]	1.153	3.818	6.492	14.190	2.330	2.657

Table 2. Hardness parameter  $\frac{1}{\rho}$  [ $10^{10}$  m] for all used interaction pairs.

	Li	Na	K	Rb	N	O
Li	3.340	3.320	*	*	3.455	3.234
Na	3.320	3.300	3.280	3.200	3.440	3.200
K	*	3.280	3.240	*	3.410	3.150
Rb	*	3.200	*	3.049	3.400	3.120
N	3.455	3.440	3.410	3.400	3.030	4.000
O	3.234	3.200	3.150	3.120	4.000	3.400

et al. [2]. These parameters reproduce the pair-correlation functions [3], and the parameters  $z_{i,j}$  and  $n_{i,j}$  guarantee the electroneutrality. The values of the parameters are listed in Table 1 and Table 2.

The interaction potential of the oxygen-atoms was extended by some Van-der-Waals-type attraction to improve the calculated pressure and self diffusion coefficients:

$$V_{\text{ext}} = \begin{cases} -\frac{27}{256} & \text{for } r < \frac{2\sigma f}{\sqrt{3}}, \\ \left( \left( \frac{\sigma f}{r} \right)^8 - \left( \frac{\sigma f}{r} \right)^6 \right) \tau & \text{for } r > \frac{2\sigma f}{\sqrt{3}}. \end{cases} \quad (2)$$

$\tau$  is fitted using the pressure values of the simulations of pure  $\text{NaNO}_3$  at 623 K and  $f$  is taken to be 0.7.

The self diffusion coefficients (SDCs) were calculated from the mean square displacements (MSD) according to the Einstein equation

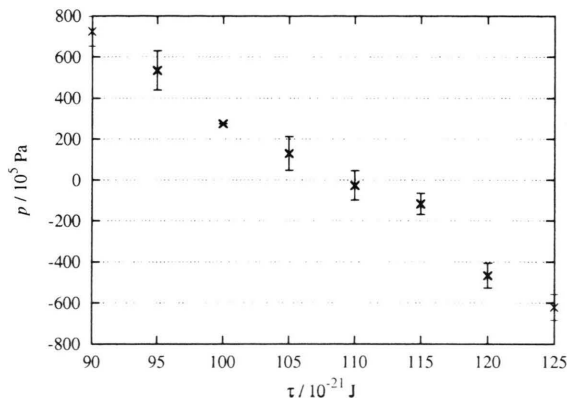
$$D = \frac{1}{6t} \left\langle |\mathbf{r}_i(t + t_0) - \mathbf{r}_i(t_0)|^2 \right\rangle. \quad (3)$$

$t$  is a sufficiently long period for the MSD to become a linear function of  $t$ , the angle brackets denote the average over the ions (cation or anions) and time origins  $t_0$ ,  $\mathbf{r}_i$  is the position of ion  $i$ .

The pressure was calculated by derivation of the potential energy with respect to the volume at fixed temperature [16, 17]. Intramolecular distances, i.e. the N-O-bondlengths in the nitrate ion, are unaffected by

Table 3. Influence of the energy parameter  $\tau$  on the pressure.

$\tau$ [ $10^{-21}$ J]	$T$ [K]	$\Delta T$ [K]	$p$ [bar]	$\Delta p$ [bar]
90	619.29	0.56	723.73	72.83
95	613.64	0.57	533.78	95.25
100	613.89	0.54	273.32	—
105	619.31	0.13	129.32	82.31
110	621.72	0.82	-28.01	71.99
115	623.41	0.53	-118.39	51.53
120	620.20	1.23	-466.99	60.14
125	615.50	0.72	-621.90	63.19

Fig. 1. Pressure vs. parameter  $\tau$  in pure  $\text{NaNO}_3$ .

volume derivation; this means that only the distances between the centers of mass have to be taken into account while calculating the derivative of the potential energy. Therefore the derivative of the Ewald-summation of the Coulomb interactions is quite lengthy. For more details see [18].

### 3. Adjusting the Potential

The energy parameter  $\tau$  of the extension of the interaction potential (2) was adjusted using simulations of pure sodium nitrate (see Fig. 1 and Table 3). The results were used in all other simulations. Except of the pressure and total energy of the system, the results of the simulations were nearly unaffected by this extension.

### 4. Results and Discussion

Since originally mixtures of different lithium isotopes were to be examined, special interest was paid to the mass dependence of the dynamics of the cations. Figure 2 shows the velocity autocorrelation function (VAC) of the cations in the four different pure

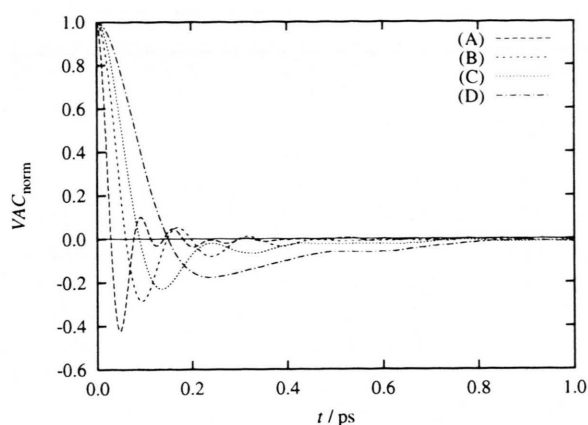


Fig. 2. Velocity autocorrelation function (VAC) of the cations in pure melts at 623 K; (A) LiNO<sub>3</sub>, (B) NaNO<sub>3</sub>, (C) KNO<sub>3</sub>, (D) RbNO<sub>3</sub>.

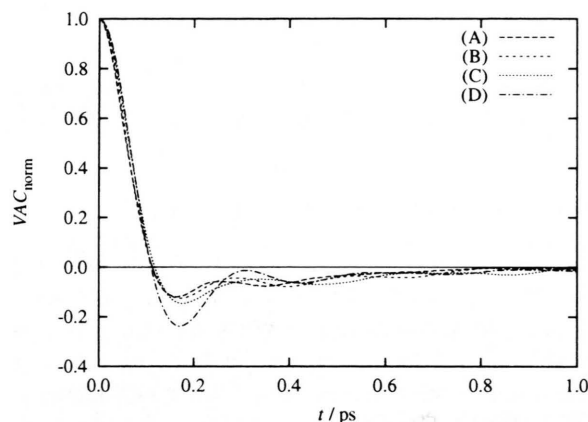


Fig. 3. VAC of the anions in pure melts at 623 K; (A) LiNO<sub>3</sub>, (B) NaNO<sub>3</sub>, (C) KNO<sub>3</sub>, (D) RbNO<sub>3</sub>.

molten salts. As expected, the VAC of the lightest ion (Li<sup>+</sup>) shows several oscillations while the VAC of the heaviest ion (Rb<sup>+</sup>) converges against zero without considerable oscillation. This effect is clearly a consequence of the different masses of the ions, confirmed by the VAC of the anions (Fig. 3): in RbNO<sub>3</sub> there is some kind of oscillation, because the rubidium ion is the only one with greater mass than the nitrate ion; all other cations under examination are lighter than the nitrate ions and are thus unable to impose a greater change in the nitrate ions' momentum.

The SDCs of the cations in the pure melts show a clear dependence on the type of the cation (Fig. 4, Table 4). Is this effect mass-dominated or size-dominated? One great advantage of computer simulation is

Table 4. SDC in several pure melts at 623 K.

Cation	$D_{\text{Cation}}$ [10 <sup>-9</sup> m <sup>2</sup> s <sup>-1</sup> ]	$\Delta D_{\text{Cation}}$	$D_{\text{Anion}}$ [10 <sup>-9</sup> m <sup>2</sup> s <sup>-1</sup> ]	$\Delta D_{\text{Anion}}$
Li	2.64	0.08	1.36	0.13
Na	1.96	0.48	1.61	0.25
K	1.45	0.21	1.59	0.21
Rb	0.93	0.03	1.02	0.04
Li (10 × mass)	2.68	0.23	—	—
Rb (mass / 10)	—	—	1.66	0.30

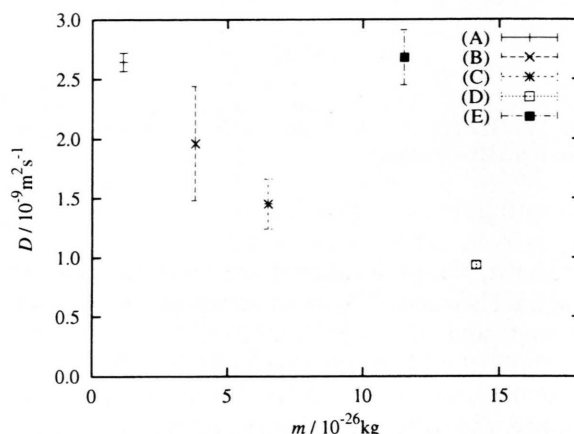


Fig. 4. Self diffusion coefficient (SDC) vs. mass of the cations; (A) Li, (B) Na, (C) K, (D) Rb, (E) Li with tenfold mass.

the possibility to exaggerate some physical properties to show characteristics otherwise unobservable. In this case a heavy Li-“isotope” was simulated, which has a mass that was arbitrarily chosen to be 10 times higher than the original Li. The two “isotopes” show a different type of motion through the fluid (see the trajectories in Fig. 5): the lighter “isotope” bounces to and fro in a cage of relatively heavy nitrate ions while the heavy “isotope” moves without these oscillations. In spite of the different motions, the SDC of the heavy “isotope” is within error bars unaffected by

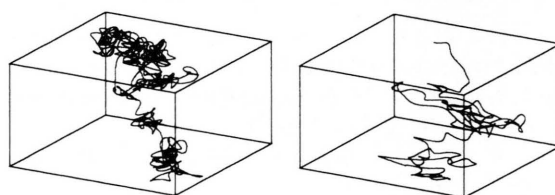


Fig. 5. Trajectories of normal (left) and “heavy” lithium (right).

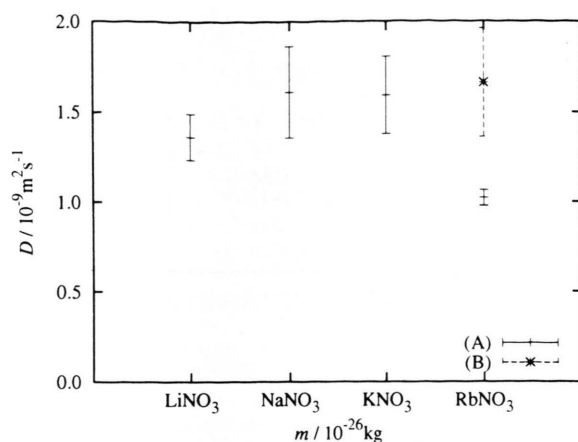


Fig. 6. SDC of nitrate in pure melts; (A) real cations, (B) light Rb-"isotope".

the change of mass. Self diffusion is therefore dominated by the radius of the ion, not, as stated in [8], by the mass. The probability of finding some "hole" in the fluid is responsible for the speed of self diffusion of small ions.

The SDCs of the nitrate ions do not show such a clear dependence (see Fig. 6): with increasing atomic number the SDC increases, too, but for RbNO<sub>3</sub> the SDC is significantly smaller. A simulation of some Rb "isotope" with 1/10th the mass of the real rubidium ion shows a SDC of the same magnitude as in the simulations with the lighter cations. This leads to the conclusion that the transport of the nitrate ion is dominated by the mass relation between cation and anion: as soon as the mass of the cation becomes greater than the mass of the anion (as in "normal" RbNO<sub>3</sub>), the anion is stuck in a "cage" of the heavier cations and its SDC decreases significantly.

From these results it is clear that the natural lithium isotopes with a mass difference of only 17 % (a *quantité négligeable* compared to the 1000% in the simulation with the artificial isotope mentioned above) cannot have different SDCs in the simulations. As long as the radius of the ion is unaffected by the

nuclear mass of the isotope, the performed simulations suggest that the SDCs of both isotopes should be the same also in reality.

## 5. Conclusions

We have carried out MD simulations of molten alkali nitrates, described by Coulomb pair potentials with Born-type repulsion and Van-der-Waals like attraction between the oxygen atoms of the nitrate ion. The latter part of the interaction potential was adapted by evaluation of the pressure in the used ensemble. The simulations describe quite well both static and dynamic properties [11, 12, 19] of the melt.

Our original ambition to explain the measured discrepancy in the cations' self diffusion coefficients in mixtures of <sup>6</sup>LiNO<sub>3</sub> and <sup>7</sup>LiNO<sub>3</sub> [ 9] could not be achieved because the mass of the cation showed no influence on the cation's self diffusion coefficient. Though the way of the cation's motion is dominated by the mass of the cation (which can be seen in the velocity autocorrelation functions) the mean square displacement even of an artificial Li-isotope with ten-fold mass shows no observable difference; therefore the mean square displacement is governed by the size of the cation. These results suggest that differences in self diffusion coefficients of light cation isotopes do not exist.

The self diffusion coefficient of the nitrate ion is affected by the mass of the cation: as soon as the nitrate's mass is smaller than the cation's mass the self diffusion of the anion is slowed down considerably. This effect is clarified by simulation of RbNO<sub>3</sub> with the mass of Rb reduced to one tenth: the self diffusion coefficient is significantly higher than that in the original RbNO<sub>3</sub>.

## Acknowledgement

Financial support by the Minister für Schule, Wissenschaft und Forschung des Landes Nordrhein-Westfalen, Düsseldorf, and the Fonds der Chemischen Industrie, Frankfurt, is gratefully acknowledged.

- [1] H. M. H. van Wechem, Thesis, Amsterdam, 1976.
- [2] T. Yamaguchi, I. Okada, H. Ohtaki, M. Mikami, and K. Kawamura, Mol. Phys. **58**, 349 (1986).
- [3] A. K. Adya, R. Takagi, and K. Kawamura, Mol. Phys. **62**, 227 (1987).
- [4] T. Kato, K. Machida, M. Oobatake, and S. Hayashi, J. Chem. Phys. **89**, 3211 (1989).
- [5] T. Kato, K. Machida, M. Oobatake, and S. Hayashi, J. Chem. Phys. **89**, 7471 (1989).
- [6] T. Kato, K. Machida, M. Oobatake, and S. Hayashi, J. Chem. Phys. **92**, 5506 (1990).
- [7] T. Kato, K. Machida, M. Oobatake, and S. Hayashi, J. Chem. Phys. **93**, 3970 (1990).

- [8] T. Kato, K. Machida, M. Oobatake, and S. Hayashi, *J. Chem. Phys.* **99**, 3966 (1993).
- [9] C. Herdlicka, J. Richter, and M. D. Zeidler, *Z. Naturforsch.* **43a**, 1075 (1988).
- [10] C. Herdlicka, J. Richter, and M. D. Zeidler, *Z. Naturforsch.* **47a**, 1047 (1992).
- [11] U. Matenaar, J. Richter, and M. D. Zeidler, *Magn. Reson. A* **122**, 72 (1996).
- [12] G. Palmer, Thesis, in preparation.
- [13] G. J. Janz, *Molten Salts Handbook*, Academic Press, London 1967, p. 202.
- [14] P. P. Ewald, *Ann. Phys.* **64**, 253 (1921).
- [15] M. Svanberg, *Mol. Phys.* **92**, 1085 (1997).
- [16] G. Hummer and N. Grønbaek-Jensen, *J. Chem. Phys.* **109**, 2791 (1998).
- [17] R. Lustig, *J. Chem. Phys.* **100**, 3048 (1994).
- [18] G. R. Vöhringer, *Molekulardynamische Simulation von Salzschnmelzen*, Thesis RWTH Aachen 2000. Online: [http://sylvester.bth.rwth-aachen.de/dissertationen/2000/3/00\\_3.pdf](http://sylvester.bth.rwth-aachen.de/dissertationen/2000/3/00_3.pdf)
- [19] A. S. Dworkin, R. B. Escue, and E. R. van Artsdalen, *J. Chem. Phys.* **64**, 872 (1960).